High Temperatures-High Pressures, Vol. 50, pp. 105–119
Reprints available directly from the publisher
Photocopying permitted by license only
DOI: 10.32908/hthp.v50.957

Thermal expansion, heat capacity and Grüneisen parameter of grossular at high temperature and high pressure

CHANG SU[1,2] AND YONGGANG LIU[3]*

[1]*School of Earth Sciences, Institute of Disaster Prevention, Sanhe-065201, China*
[2]*Hebei Key Laboratory of Earthquake Dynamics, Sanhe-065201, China*
[3]*Key Laboratory for High Temperature and High Pressure Study of the Earth's Interior, Institute of Geochemistry, Chinese Academy of Science, Guiyang–550081, China*

Received: February 25, 2020; Accepted: August 15, 2020.

The thermodynamic properties of grossular garnet ($Ca_3Al_2Si_3O_{12}$) were determined as a function of pressure and temperature in this study. With a numerical iterative procedure, the unit-cell volume, adiabatic bulk modulus, thermal expansion, heat capacity, and Grüneisen parameters of grossular up to 25 GPa, 2000 K were extracted from experimental elastic wave velocities at high temperature and high pressure conditions. The calculated unit-cell volume and adiabatic bulk modulus agree well with the previous studies. The results imply that our calculated thermal expansion, heat capacity, and Grüneisen parameters of grossular are all decrease with elevated pressure, and both thermal expansion and heat capacity show nonlinear pressure dependences. On the other hand, the Grüneisen parameter shows a linear pressure dependence. The pressure derivative of thermal expansion display a regularity increase with temperature, while the pressure derivatives of heat capacity and Grüneisen parameters display a rapid decrease at low temperature and a slow growth above ∼1000 K.

Keywords: Grossular, Thermodynamic parameters, High-temperature High-pressure, Elastic wave velocity

*Corresponding author: liuyonggang@vip.gyig.ac.cn

1 INTRODUCTION

Garnet is assumed to be one of the most abundant constituent minerals. In pyrolite model, the volume fraction of garnet in the uppermost mantle is ∼15 %, then increases to ∼40 % with increasing depth to the mantle transition zone, while in eclogite model, the volume fraction increases from ∼25 % in the uppermost mantle to ∼70 % in the mantle transition zone [1–3].

Elastic properties of mantle minerals at high temperature and high pressure conditions are essential to understanding the properties of the Earth's interior [4]. Because of garnet's relatively high density, low compressibility, and increasing stability with increasing pressure, various of high temperature and high pressure experimental investigations have provided us plenty of accurate data as unit-cell volume [5–11] and elastic wave velocity [12–14], from which the elastic properties of garnet in a wide range of temperature and pressure were determined to constrain the compositions of the lower crust, upper mantle and transition zone [15–17].

However, comparing to the sufficient elastic moduli and volume data of garnet, data of thermodynamic properties of garnet, especially at high pressure conditions, is lacking. Thermodynamic properties such as thermal expansion, heat capacity, and Grüneisen parameter are essential parameters in both geodynamics and mineral physics [18]. Moreover, because garnet exists in a wide range of depth in the Earth's interior, it's suggested to be one of the most common inclusions in diamond [19]. And since diamond is a mantle-derived mineral, its absolute ages are usually used to provide records of the deep geological process [20,21]. Hence, the determination of the thermodynamic properties of garnet at high temperature and high pressure conditions is significant in understanding the physical environment in which the garnet and its host, inclusion-bearing diamond, formed [19,22].

As we know, thermal expansions of minerals can be deduced from experimental measurements on volume [23,24], but heat capacity could only be measured by calorimetry at either ambient pressure or less than 2 GPa [25–28]. The first-principle calculation is a well-accepted method to obtain high pressure thermodynamic properties of minerals [3,29], and Osako et al. [30] presented an experimental approach to get the high pressure heat capacity by measuring the thermal conductivity and thermal diffusivity simultaneously. Still, a lot of work needs to be done to deal with the lack of thermodynamic data of numerous minerals.

In 1967, Davis and Gordon [31] introduced a numerical iterative procedure, following which the density, thermal expansion and heat capacity, especially, at high temperature and high pressure conditions could be obtained from adiabatic elastic wave velocities. The feasibility of this method has been proved on liquids [32–34] solutions [35] and recently, on solid minerals [36]. Thus, with the available numerous experimental data of minerals, the

thermodynamic properties at high pressure conditions can be determined conveniently.

As a representative end-member mineral of the garnet group, grossular ($Ca_3Al_2Si_3O_{12}$) is an essential component in the carbonate-bearing ultrahigh-pressure eclogites [37]. Though there is a sufficient amount of data on the volume, elastic properties of grossular, the high pressure thermodynamic properties of grossular have only been obtained by the first-principles calculations to date. In this study, made use of this theoretical method and existing high temperature and high pressure elastic wave velocities of grossular, we reported the pressure and temperature dependence of the unit-cell volume, elastic properties and thermodynamic properties of grossular up to 25 GPa and 2000 K. To testify the accuracy of our results, comparisons with previous works were made. In addition, we also studied the temperature and pressure derivatives of thermal expansion, heat capacity, and Grüneisen parameters of grossular.

2 CALCULATION PROCEDURE

2.1 Theoretical method

This method is based on a series of classical thermodynamic relations, and the fundamental equations are shown below [31, 32].

The thermal expansion (α) is defined as the temperature dependence of volume (V), which is expressed by:

$$\alpha = \frac{1}{V}\left(\frac{\partial V}{\partial T}\right)_P \tag{1}$$

Also, the isothermal bulk modulus ($K_T = \rho(\partial\rho / \partial P)_T$) and adiabatic bulk modulus ($K_S = \rho v_B^2$) are related to the sound velocity by:

$$\frac{1}{K_T} = \frac{1}{K_S} + \frac{VT\alpha^2}{C_P} \tag{2}$$

where v_B stands for bulk velocity, which is related to P-wave velocity (v_P) and S-wave velocity (v_s) as:

$$v_B = \left(v_p^2 - \frac{4}{3}v_s^2\right)^{\frac{1}{2}} \tag{3}$$

Hence,

$$\left(\frac{\partial V}{\partial P}\right)_T = -V^2\left(\frac{1}{v_B^2} + \frac{T\alpha^2}{C_P}\right) \tag{4}$$

According to the definition of isobaric heat capacity (C_P), its variation with pressure can be evaluated by:

$$\left(\frac{\partial C_P}{\partial P}\right)_T = -VT\left[\alpha^2 + \left(\frac{\partial \alpha}{\partial T}\right)_P\right] \tag{5}$$

To start the calculation, first, we get the fitting equation of V as a function of temperature at zero pressure $V(P_0, T)$ to obtain α (α_0, T) at ambient pressure by Eq. (1). With α (α_0, T) and the relationship between C_P and temperature at ambient pressure $C_P(P_0, T)$, the approximate V at an arbitrary reference pressure could be estimated using Eq. (4). Then resulting V is used to update the value of α and C_P at the same pressure with Eq. (1) and (5), respectively. Iteration of this loop leads to converged values of V, α and C_P at high pressure conditions based on experimental elastic wave velocity.

In spite of V, α and C_P, another derived thermodynamic quantity is the Grüneisen parameter (γ) [3]:

$$\gamma = \frac{\alpha K_S \mathrm{V}}{C_P} \tag{6}$$

Hence the unit-cell volume, thermal expansion, heat capacity, and Grüneisen parameter as a function of pressure and temperature can be extracted.

2.2 Data of mantle minerals from previous work

2.2.1 Volume at high temperature and ambient pressure

The unit-cell volume of grossular at ambient condition has been measured by X-ray diffraction [5,38], which provides an average value as 1663.16 ± 1.06 Å. Using a horizontal differential dilatometer, Isaak et al. [39] measured the high temperature thermal expansion of grossular to 1350 K, as well as the estimated values to 2000 K. In this paper, they also provide the density of grossular at ambient conditions. Though later, Saxena et al. [40] presented the fitting equation for the ambient pressure thermal expansion of grossular as a function of temperature to ∼3000 K, which was obtained from the experimental data by Anderson et al. [41]. The value by Saxena [40] consistent with that by Isaak [39] at 500 K, however, was ∼8 % and even ∼21 % lower than that Isaak et al. [39] at 1000 K and 2000 K, respectively. Recently, Milani et al. [11] measured the ambient pressure unit-cell volumes of grossular to 1030 K by X-ray diffraction, and separation of thermal expansion was only 1.5 % compared to that by Isaak [39] at 1000 K. Since the temperature range in this study is from 300 K to 2000 K, thus here we made use of the data by Isaak et al. [39].

2.2.2 Heat capacity at high temperature and ambient pressure

Heat capacity of grossular was determined using calorimetry up to 1000 K [42–44], then the fitting equation of experimental heat capacity as a function of temperature has been refined by Saxena et al. [40]. Later, Thiéblot et al. [45] measured the heat capacities of synthetic grossular from drop-calorimetry measurements between 400 K and 1390 K and fit the data to the Haas and

Fisher equation [46], which provided a C_P-T relation to ~1000 K. However, calculated data using the fitting equation provided by Thiéblot gave a slight decrease over ~1200 K, which seems unreasonable, thus in this study, we make use of the C_P-T equation by Saxene et al. [40].

2.2.3 Elastic wave velocity at high temperature and high pressure

The ambient pressure elastic wave velocities of grossular with increasing temperature have been directly measured using Brillouin scattering [47] and derived from experimental elasticity data measured by the rectangular parallelepiped resonance method [39]. Then using ultrasonic measurements, the elastic wave velocities to 17 GPa and 1650 K were determined by Kono et al. [13]. Later, Gwanmesia et al. [14] also provided the elastic wave velocities in the lower pressure range, which covered the data below 5 GPa. Since the measured [12–14] v_P and v_S of grossular at ambient conditions were consistent with that by Isaak et al. [39] but ~35 % and ~40 %, respectively, larger than that by Askarpour et al. [47], in this study, we made use of the data by Isaak et al. [39], Kono et al. [13] and Gwanmesia et al. [14].

During the calculation process, the fitting equation of elastic velocities of grossular as functions of temperature and pressure are needed to calculate the P-wave velocity and S-wave velocity at small temperature and pressure intervals. Since the elastic wave velocities of grossular were suggested to be linear with pressure and temperature up to 17 GPa, 1650 K [13]. Hence, with the combination of ambient and high pressure data [13,14,39], we fitted the elastic wave velocity as a function of both temperature and pressure with a linear fitting equation, which is shown in Eq. (7), together with the coefficients listed in Table 1.

$$v(P,T) = a_0 T + a_1 P + a_2 \tag{7}$$

TABLE 1
Coefficients for Eq. (7) with v in m/s, T in K and P in GPa, together with the R^2

	a_0	a_1	a_2	R^2
v_p	-0.42 ± 0.01	66.71 ± 0.55	9451.63 ± 6.79	0.996
v_s	-0.30 ± 0.01	19.24 ± 0.49	5546.30 ± 6.11	0.994

3 RESULTS AND DISCUSSION

3.1 Unit-cell volume at high temperature and high pressure conditions

Using the data listed above and based on Eq.(1) and Eq.(3)–(5), our calculation results for the volume of grossular to 20 GPa, 2000 K is shown in Figure 1 along with previous studies for comparison.

Unit-cell volume of grossular was obtained by experimental [5–11, 38] and theoretical method [10,48]. At room temperature, though, our results are

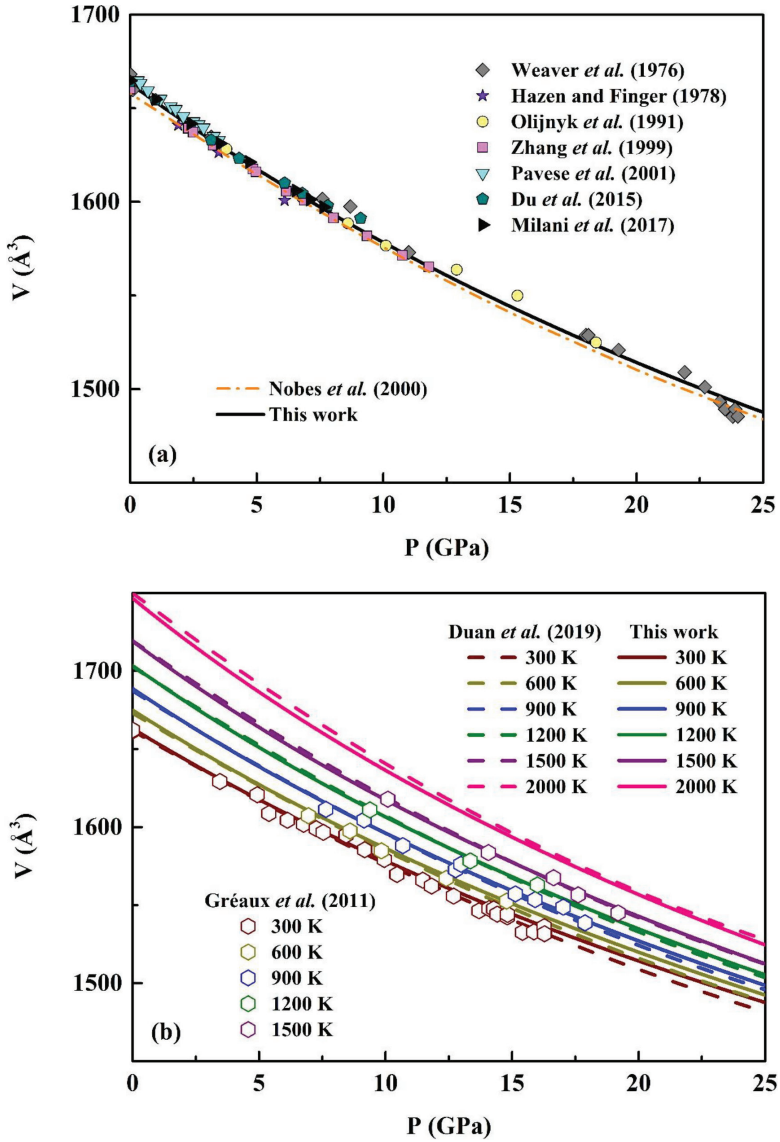

FIGURE 1
Unit-cell volume of grossular as a function of pressure at room temperature (a) and high temperatures (b).

~0.2 % lower than that by Pavese et al. [8] and ~0.2 % higher than that by Nobes et al. [48], they generally agree well with experimental results below ~12 GPa [5–7,9–11,38]. High temperature and high pressure unit-cell volumes were determined by Gréaux et al. [9] and Duan et al. [3] using X-ray

diffraction and first-principle calculations, respectively. Our result is slightly larger than that by Duan et al. [3] and the difference increases with temperature, with the largest separation as 0.3 % at 2000 K.

3.2 Adiabatic bulk modulus at high temperature and high pressure conditions

The adiabatic bulk modulus of grossular is presented in Figure 2, together with the previous experimental [12–14] and theoretical [3] results.

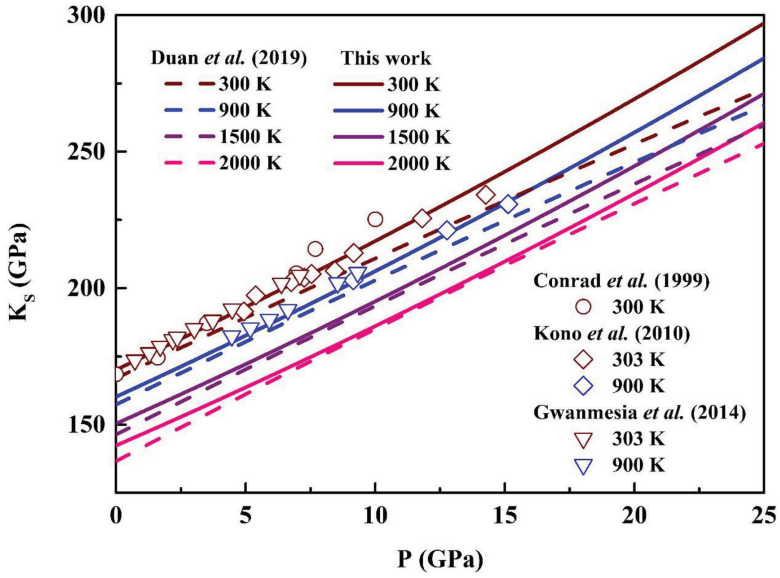

FIGURE 2
Adiabatic bulk modulus and shear modulus variations with pressure at different temperatures.

To obtain the pressure derivatives of the adiabatic bulk modulus $(\partial K_S/\partial P)_T$ and the temperature derivatives of the adiabatic bulk modulus $(\partial K_S/\partial T)_P$, we fitted the calculated high temperature and high pressure K_S using the third-order finite strain equation [49–51]:

$$K_S(T) = K_{S0}(1+2f)^{5/2}\left\{1+\left[3(\partial K_S/\partial P)_T - 5\right]f\right\} \tag{8}$$

$$K_{S0} = K_{S0}(300\,K) + (\partial K_S/\partial T)_P (T-300) \tag{9}$$

where $f = (1/2)\{[V_0(T)/V]^{2/3} - 1\}$, $K_S(T)$ is the adiabatic bulk modulus at temperature T and high pressure, $K_{S0}(T)$ is the adiabatic bulk modulus at temperature T and ambient pressure. The results are summarized in Table 2.

TABLE 2
Adiabatic bulk modulus and its first pressure and temperature derivative of grossular

K_{S0} (300 K) GPa	$(\partial K_S/\partial P)_{300\,K}$	$(\partial K_S/\partial T)_P$ GPa K^{-1}	Method	References
166.82	5.46	–	Brillouin scattering	Conrad et al. (1999)
171.5	4.42	−0.0136	Ultrasonic wave velocity	Kono et al. (2010)
171.2	4.47	−0.0138	Ultrasonic interferometry	Gwanmesia et al. (2015)
167.03	4.49*	−0.0141	Theoretically	Duan et al. (2019)
170.13	4.43	−0.0164	Theoretically	This work

*$\partial^2 K_S/\partial P^2 = -10.2 \times 10^{-3}\ GPa^{-1}$

In Figure 2, our data is comparable with those experimental results [12–14], and the good agreement with the data by Kono at al. [13] and Gwanmesia et al. [14] confirms the accuracy of our derived unit-cell volumes at high temperature and high pressure conditions. The pressure derivatives of K_S in this study are generally larger than that by Duan et al. [3]. The values of $(\partial K_S/\partial P)_T$ increase from 4.43 at ambient pressure to 5.53 at 25 GPa at the temperature of 300 K, and decrease from 4.43 at 300 K to 3.84 at 2000 K at ambient pressure.

3.3 Thermodynamic properties at high temperature and high pressure conditions

The good agreement of the calculated unit-cell volume and adiabatic bulk modulus with previous studies consequently lead to the reliability of the calculated thermodynamic properties of grossular. Figure 3, Figure 4 and Figure 6 illustrate the calculated thermal expansions, heat capacities and Grüneisen parameters of grossular at high pressure conditions, respectively.

Though thermodynamic properties of grossular have been well studied at ambient pressure conditions, their values at high pressure conditions are still lacking. The only source we could find about the thermodynamic properties of grossular at the high pressure conditions is obtained from first-principle calculations [3]. Our thermal expansion and heat capacity are agreed with the first-principle calculations results [3]. The calculated thermal expansions and heat capacities of grossular are fitted to the equations $\alpha = \alpha_0 + (\partial\alpha/\partial P) \times P + (\partial^2\alpha/\partial P^2) \times P^2$ and $C_P = C_{P0} + (\partial C_P/\partial P) \times P + (\partial^2 C_P/\partial P^2) \times P^2$ at fixed temperatures, respectively, where α_0 and C_{P0} stand for the thermal expansion and heat capacity at ambient pressure, respectively, $\partial\alpha/\partial P$, $\partial^2\alpha/\partial P^2$, $\partial C_P/\partial P$, $\partial^2 C_P/\partial P^2$ stand for the first and second pressure derivatives of thermal expansion or heat capacity, respectively. All the fitting parameters are listed in Table 3 and Table 4, and the estimated heat capacity and its pressure derivative at 300 K are comparable with that by Watanabe et al. [30,52]. The results suggest that both of thermal expansion and heat capacity show

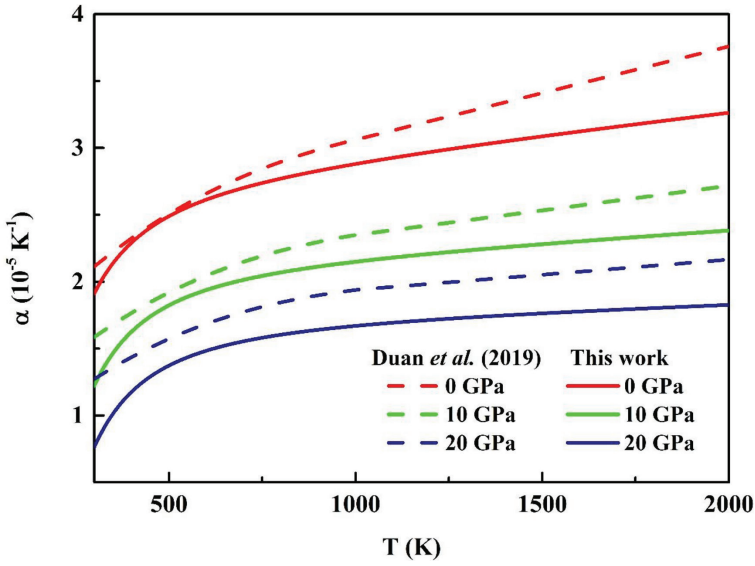

FIGURE 3
Thermal expansion of grossular as a function of temperature at various pressures.

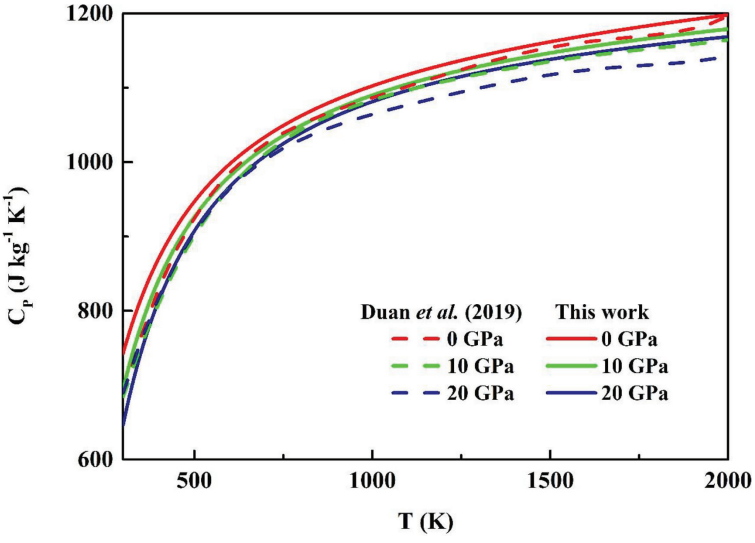

FIGURE 4
Heat capacity of grossular as a function of temperature at various pressures.

nonlinear pressure dependences and also decrease with elevated pressure. Furthermore, the pressure effect on the thermal expansion increase with temperature, however, the pressure effect on the heat capacity does not show

TABLE 3
Thermal expansion and its first, second pressure derivatives of grossular

T	α_0	$\partial\alpha/\partial P$	$\partial^2\alpha/\partial P^2$
K	$10^{-5}K^{-1}$	$10^{-7}K^{-1}GPa^{-1}$	$10^{-8}K^{-1}GPa^{-2}$
300	1.911	−7.629	0.989
600	2.612	−7.562	0.980
900	2.828	−7.995	1.060
1200	2.969	−8.500	1.152
1500	3.086	−9.024	1.247
2000	3.262	−9.913	1.408

TABLE 4
Heat capacity and its first, second pressure derivatives of grossular

T	C_{P0}	$\partial C_P/\partial P$	$\partial^2 C_P/\partial P^2$	References
K	$J\,kg^{-1}K^{-1}$	$J\,kg^{-1}K^{-1}GPa^{-1}$	$10^{-2}\,J\,kg^{-1}K^{-1}GPa^{-2}$	
300	706	−3.1	–	Watanabe et al. (1982)
300	742.94	−4.87	0.3	This work
600	997.57	−1.71	0.95	This work
900	1084.36	−1.38	1.51	This work
1200	1130.45	−1.47	2.08	This work
1500	1161.20	−1.69	2.68	This work
2000	1197.30	−2.19	3.73	This work

regularity with the temperature. Figure 5 illustrates the relationship between the first pressure derivative of heat capacity and temperature, the value of $\partial C_P/\partial P$ seems to decrease rapidly below ∼500 K, then starts to increase over ∼1000 K.

Finally, the Grüneisen parameter of grossular at high temperature and high pressure conditions can be obtained in terms of the calculated adiabatic bulk modulus, thermal expansion and heat capacity. The results are presented in Figure 6, together with the ambient pressure values to 1200 K by Isaak et al. [39]. The calculated Grüneisen parameter shows a linear pressure dependence, and the pressure derivative of the Grüneisen parameter displays a similar trend with that of heat capacity, which is also illustrated in Figure 5.

Additionally, our calculated Grüneisen parameters decrease with elevated pressure and also show a slight decrease with elevated temperature. The temperature derivatives of the Grüneisen parameter increase from $-4.9 \times 10^{-5}\,K^{-1}$ at 0 GPa to $-5.4 \times 10^{-5}\,K^{-1}$ at 20 GPa over ∼750 K, which displays the same

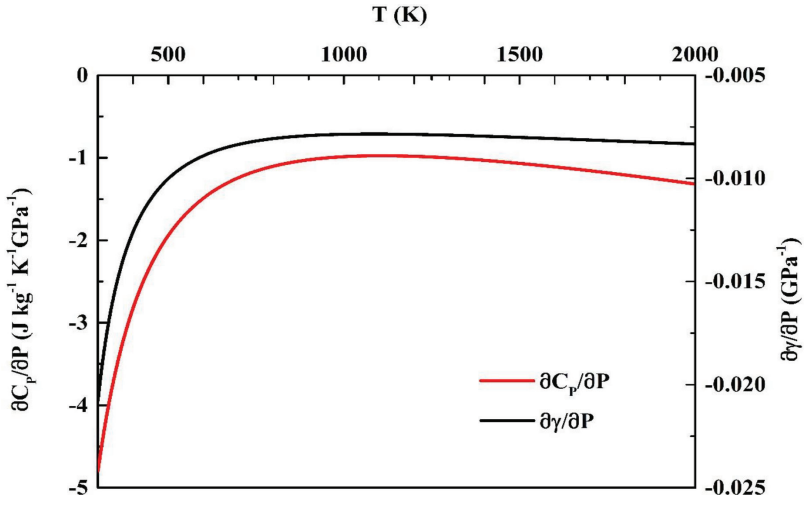

FIGURE 5
Pressure derivative of heat capacity and Grüneisen parameter of grossular variations with temperature.

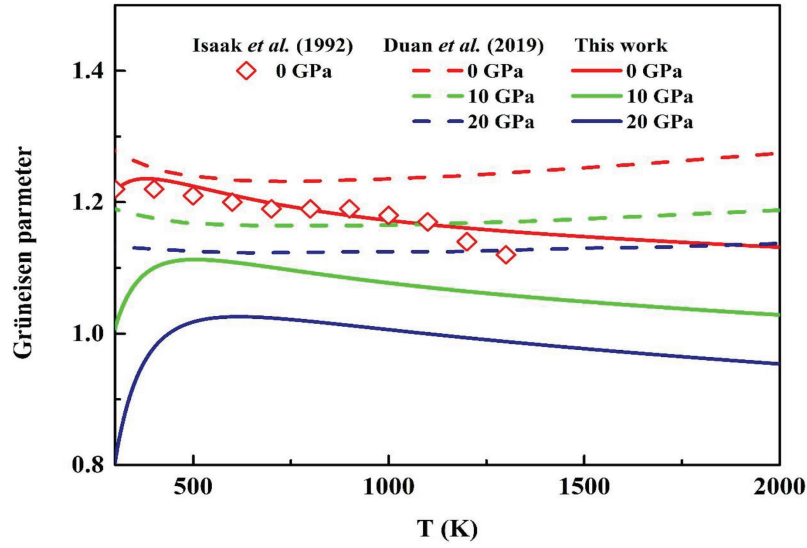

FIGURE 6
Grüneisen parameters of grossular as a function of temperature at various pressures.

trend with the data by Isaak et al. [39]. However, based on the relationship between Grüneisen parameter and volume, previous studies suggest that the Grüneisen parameter at high temperature and high pressure conditions increasing with increasing temperature and decreasing upon compression

[11,53,54]. Hence, the temperature derivative of the Grüneisen parameter of grossular at high temperature and high pressure conditions still need to be discussed in future studies.

4 CONCLUSIONS

Based on the previous high temperature and high pressure experimental elastic wave velocity data, the unit-cell volume, adiabatic bulk modulus and particularly, thermodynamic parameters including thermal expansion, heat capacity and Grüneisen parameter of grossular up to 25 GPa, 2000 K were obtained following a numerical iterative procedure. Both of the unit-cell volume and adiabatic bulk modulus agree well with previous experimental investigations, which consequently proved the reliability of our theoretical method. The temperature and pressure dependences of those thermodynamic parameters were studied and the results suggest that the thermal expansion, heat capacity and Grüneisen parameter of grossular are all decease with pressure. Also, both of the thermal expansion and heat capacity show nonlinear pressure dependence while the Grüneisen parameter shows a linear pressure dependence. Additionally, the pressure derivative of heat capacity displays an interesting trend with the temperature that the value shows a steep decrease to $\sim$500 K, then a slow increase above $\sim$1000 K. In this study, the temperature derivative of the calculated Grüneisen parameter is negative, which is in contrast to the previous studies.

ACKNOWLEDGEMENTS

This work was supported by the Fundamental Research Funds for the Central Universities, SCUT (ZY20180234), and the National Natural Science Foundation of China (Grant No. 41873075).

REFERENCES

[1] Bass, J.D. and D.L. Anderson, Composition of the upper mantle: Geophysical tests of two petrological models. Geophysical Research Letters, 1984. 11(3): p. 229–232. DOI: 10.1029/GL011i003p00229.

[2] Irifune, T. and A.E. Ringwood, Phase transformations in a harzburgite composition to 26 GPa: implications for dynamical behaviour of the subducting slab. Earth and Planetary Science Letters, 1987. 86(2–4): p. 365–376. DOI: 10.1016/0012-821x(87)90233-0.

[3] Duan, L., W. Wang, Z. Wu, and W. Qian, Thermodynamic and Elastic Properties of Grossular at High Pressures and High Temperatures: A First Principles Study. Journal of Geophysical Research: Solid Earth, 2019. 124(8): p. 7792–7805. DOI: 10.1029/2019jb017439.

[4] Bass, J.D., S.V. Sinogeikin, and B. Li, Elastic Properties of Minerals: A Key for Understanding the Composition and Temperature of Earth's Interior. Elements, 2008. 4(3): p. 165–170. DOI: 10.2113/gselements.4.3.165.

[5] Weaver, J.S., T. Takahashi, and J. Bass, Isothermal compression of grossular garnets to 250 Kbar and the effect of calcium on the bulk modulus. Journal of Geophysical Research, 1976. 81(14): p. 2475–2482. DOI: 10.1029/JB081i014p02475.
[6] Olijnyk, H., E. Paris, C.A. Geiger, and G.A. Lager, Compressional study of katoite [$Ca_3Al_2(O_4H_4)_3$] and grossular garnet. Journal of Geophysical Research: Solid Earth, 1991. 96(B9): p. 14313–14318. DOI: 10.1029/91jb01180.
[7] Zhang, L., H. Ahsbahs, A. Kutoglu, and C.A. Geiger, Single-crystal hydrostatic compression of synthetic pyrope, almandine, spessartine, grossular and andradite garnets at high pressures. Physics and Chemistry of Minerals, 1999. 27(1): p. 52–58. DOI: 10.1007/s002690050240.
[8] Pavese, A., V. Diella, V. Pischedda, M. Merli, R. Bocchio, and M. Mezouar, Pressure-volume-temperature equation of state of andradite and grossular, by high-pressure and -temperature powder diffraction. Physics and Chemistry of Minerals, 2001. 28(4): p. 242–248. DOI: 10.1007/s002690000144.
[9] Gréaux, S., Y. Kono, N. Nishiyama, T. Kunimoto, K. Wada, and T. Irifune, P–V–T equation of state of $Ca_3Al_2Si_3O_{12}$ grossular garnet. Physics and Chemistry of Minerals, 2010. 38(2): p. 85–94. DOI: 10.1007/s00269-010-0384-1.
[10] Du, W., S.M. Clark, and D. Walker, Thermo-compression of pyrope-grossular garnet solid solutions: Non-linear compositional dependence. American Mineralogist, 2014. 100(1): p. 215–222. DOI: 10.2138/am-2015-4752.
[11] Milani, S., R.J. Angel, L. Scandolo, M.L. Mazzucchelli, T.B. Ballaran, S. Klemme, M.C. Domeneghetti, R. Miletich, K.S. Scheidl, M. Derzsi, K. Tokár, M. Prencipe, M. Alvaro, and F. Nestola, Thermo-elastic behavior of grossular garnet at high pressures and temperatures. American Mineralogist, 2017. 102(4): p. 851–859. DOI: 10.2138/am-2017-5855.
[12] Conrad, P., G., C.-S. Zha, H.-K. Mao, and R. Hemley, J., The high-pressure, single-crystal elasticity of pyrope, grossular, and andradite, in American Mineralogist. 1999. p. 374. DOI: 10.2138/am-1999-0321
[13] Kono, Y., S. Gréaux, Y. Higo, H. Ohfuji, and T. Irifune, Pressure and temperature dependences of elastic properties of grossular garnet up to 17 GPa and 1650 K. Journal of Earth Science, 2010. 21(5): p. 782–791. DOI: 10.1007/s12583-010-0112-2.
[14] Gwanmesia, G.D., L. Wang, A. Heady, and R.C. Liebermann, Elasticity and sound velocities of polycrystalline grossular garnet ($Ca_3Al_2Si_3O_{12}$) at simultaneous high pressures and high temperatures. Physics of the Earth and Planetary Interiors, 2014. 228: p. 80–87. DOI: 10.1016/j.pepi.2013.09.010.
[15] Bass, J.D., Elasticity of grossular and spessartite garnets by Brillouin spectroscopy. Journal of Geophysical Research, 1989. 94(B6): p. 7621–7628. DOI: 10.1029/JB094iB06p07621.
[16] Irifune, T., Y. Higo, T. Inoue, Y. Kono, H. Ohfuji, and K. Funakoshi, Sound velocities of majorite garnet and the composition of the mantle transition region. Nature, 2008. 451(7180): p. 814–7. DOI: 10.1038/nature06551.
[17] Wood, B.J., E.S. Kiseeva, and A.K. Matzen, Garnet in the Earth's Mantle. Elements, 2013. 9(6): p. 421–426. DOI: 10.2113/gselements.9.6.421.
[18] Yoneda, A., M. Osako, and E. Ito, Heat capacity measurement under high pressure: A finite element method assessment. Physics of the Earth and Planetary Interiors, 2009. 174(1–4): p. 309–314. DOI: 10.1016/j.pepi.2008.10.004.
[19] Nestola, F., D.E. Jacob, M.G. Pamato, L. Pasqualetto, B. Oliveira, S. Greene, S. Perritt, I. Chinn, S. Milani, N. Kueter, N. Sgreva, P. Nimis, L. Secco, and J.W. Harris, Protogenetic garnet inclusions and the age of diamonds. Geology, 2019. 47(5): p. 431–434. DOI: 10.1130/g45781.1.
[20] Smith, E.M., S.B. Shirey, F. Nestola, E.S. Bullock, J. Wang, S.H. Richardson, and W. Wang, Large gem diamonds from metallic liquid in Earth's deep mantle. Science, 2016. 354(6318): p. 1403–1405. DOI: 10.1126/science.aal1303.
[21] Smith, E.M., S.B. Shirey, S.H. Richardson, F. Nestola, E.S. Bullock, J. Wang, and W. Wang, Blue boron-bearing diamonds from Earth's lower mantle. Nature, 2018. 560(7716): p. 84–87. DOI: 10.1038/s41586-018-0334-5.
[22] Milani, S., F. Nestola, M. Alvaro, D. Pasqual, M.L. Mazzucchelli, M.C. Domeneghetti, and C.A. Geiger, Diamond–garnet geobarometry: The role of garnet compressibility and expansivity. Lithos, 2015. 227: p. 140–147. DOI: 10.1016/j.lithos.2015.03.017.

[23] Anderson, O.L., Equation for thermal expansivity in planetary interiors. Journal of Geophysical Research, 1967. 72(14): p. 3661–3668. DOI: 10.1029/JZ072i014p03661.
[24] Kuang, Y., J. Xu, D. Zhao, D. Fan, X. Li, Z. Wen-Ge, and H. Xie, The high-pressure elastic properties of celestine and the high-pressure behavior of barite-type sulphates. High Temperatures-High Pressures, 2017. 46: p. 481–495.
[25] Bosenick, A., C.A. Geiger, and L. Cemič, Heat capacity measurements of synthetic pyrope-grossular garnets between 320 and 1000 K by differential scanning calorimetry. Geochimica et Cosmochimica Acta, 1996. 60(17): p. 3215–3227. DOI: 10.1016/0016-7037(96)00150-0.
[26] Andersson, S.P. and R.G. Ross, Thermal Conductivity and Heat-Capacity Per Unit Volume of Poly(Methyl Methacrylate) under High Pressure. International Journal of Thermophysics, 1994. 15(5): p. 949–962. DOI: 10.1007/Bf01447105.
[27] Kaisersberger, E., Specific heat determination by differential scanning calorimetry: Improvements through automated sample handling. High Temperatures-High Pressures, 1999. 31: p. 55–61. DOI: 10.1068/htec107.
[28] Kohli, R., Measurement of high-temperature specific heats: thermodynamics of alkali metal systems. High Temperatures-High Pressures, 1999. 31(1): p. 49–53. DOI: 10.1068/htec452.
[29] Hu, Y., Z. Wu, P.K. Dera, and C.R. Bina, Thermodynamic and elastic properties of pyrope at high pressure and high temperature by first-principles calculations. Journal of Geophysical Research: Solid Earth, 2016. 121(9): p. 6462–6476. DOI: 10.1002/2016jb013026.
[30] Osako, M., E. Ito, and A. Yoneda, Simultaneous measurements of thermal conductivity and thermal diffusivity for garnet and olivine under high pressure. Physics of the Earth and Planetary Interiors, 2004. 143–144: p. 311–320. DOI: 10.1016/j.pepi.2003.10.010.
[31] Davis, L.A. and R.B. Gordon, Compression of Mercury at High Pressure. The Journal of Chemical Physics, 1967. 46(7): p. 2650–2660. DOI: 10.1063/1.1841095.
[32] Ayrinhac, S., M. Gauthier, L.E. Bove, M. Morand, G. Le Marchand, F. Bergame, J. Philippe, and F. Decremps, Equation of state of liquid mercury to 520 K and 7 GPa from acoustic velocity measurements. J Chem Phys, 2014. 140(24): p. 244201. DOI: 10.1063/1.4882695.
[33] Li, H., X. Zhang, Y. Sun, and M. Li, Thermodynamic properties of liquid sodium under high pressure. AIP Advances, 2017. 7(4): p. 13. DOI: 10.1063/1.4980023.
[34] Su, C., Y. Liu, Z. Wang, W. Song, P.D. Asimow, H. Tang, and H. Xie, Equation of state of liquid bismuth and its melting curve from ultrasonic investigation at high pressure. Physica B: Condensed Matter, 2017. 524: p. 154–162. DOI: 10.1016/j.physb.2017.08.049.
[35] Lago, S. and P.A. Giuliano Albo, A new method to calculate the thermodynamical properties of liquids from accurate speed-of-sound measurements. The Journal of Chemical Thermodynamics, 2008. 40(11): p. 1558–1564. DOI: 10.1016/j.jct.2008.06.018.
[36] Su, C., Y. Liu, W. Song, D. Fan, Z. Wang, and H. Tang, Thermodynamic properties of San Carlos olivine at high temperature and high pressure. Acta Geochimica, 2018. 37(2): p. 171–179. DOI: 10.1007/s11631-018-0261-z.
[37] Omori, S., J.G. Liou, R.Y. Zhang, and Y. Ogasawara, Petrogenesis of impure dolomitic marble from the Dabie Mountains, central China. The Island Arc, 1998. 7(1–2): p. 98–114. DOI: 10.1046/j.1440-1738.1998.00189.x.
[38] Hazen, R.M. and L.W. Finger, Crystal structures and compressibilities of pyrope and grossular to 60 kbar. American Mineralogist, 1978. 63(3–4): p. 297–303.
[39] Isaak, D., O. Anderson, and H. Oda, High-temperature thermal expansion and elasticity of calcium-rich garnets. Physics and Chemistry of Minerals, 1992. 19(2): p. 106–120. DOI: 10.1007/bf00198608.
[40] Saxena, S.K., N. Chatterjee, Y. Fei, and G. Shen, Thermodynamic Data on Oxides and Silicates. 1993: Springer Science & Business Media.
[41] Anderson, O.L., D.L. Isaak, and H. Oda, Thermoelastic parameters for six minerals at high temperature. Journal of Geophysical Research: Solid Earth, 1991. 96(B11): p. 18037–18046. DOI: 10.1029/91jb01579.
[42] Krupka, K.M., R.A. Robie, and B.S. Hemingway, High-temperature heat capacities of corundum, periclase, anorthite, $CaAl_2Si_2O_8$ glass, muscovite, pyrophyllite, $KAlSi_3O_8$ glass, grossular, and $NaAlSi_3O_8$ glass. Am. Mineral., 1979. 64: p. 86–101.

[43] Westrum, E.F., E.J. Essene, and D. Perkins, Thermophysical properties of the garnet, grossular: $Ca_3Al_2Si_3O_{12}$. The Journal of Chemical Thermodynamics, 1979. 11(1): p. 57–66. DOI: 10.1016/0021-9614(79)90083-1.

[44] Haselton, H.T. and E.F. Westrum, Low-temperature heat capacities of synthetic pyrope, grossular, and pyrope60grossular40. Geochimica et Cosmochimica Acta, 1980. 44(5): p. 701–709. DOI: 10.1016/0016-7037(80)90159-3.

[45] Thiéblot, L., C. Téqui, and P. Richet, High-temperature heat capacity of grossular ($Ca_3Al_2Si_3O_{12}$), enstatite ($MgSiO_3$), and titanite ($CaTiSiO_5$), in American Mineralogist. 1999. p. 848. DOI: 10.2138/am-1999-5-619.

[46] Haas, J.L. and J.R. Fisher, Simultaneous evaluation and correlation of thermodynamic data. American Journal of Science, 1976. 276(4): p. 525–545. DOI: 10.2475/ajs.276.4.525.

[47] Askarpour, V., M.H. Manghnani, and P. Richet, Elastic properties of diopside, anorthite, and grossular glasses and liquids: A Brillouin Scattering study up to 1400 K. Journal of Geophysical Research: Solid Earth, 1993. 98(B10): p. 17683–17689. DOI: 10.1029/93jb01558.

[48] Nobes, R.H., E.V. Akhmatskaya, V. Milman, B. Winkler, and C.J. Pickard, Structure and properties of aluminosilicate garnets and katoite: an ab initio study. Computational Materials Science, 2000. 17(2–4): p. 141–145. DOI: 10.1016/s0927-0256(00)00011-2.

[49] Fan, D., S. Fu, J. Yang, S.N. Tkachev, V.B. Prakapenka, and J.-F. Lin, Elasticity of single-crystal periclase at high pressure and temperature: The effect of iron on the elasticity and seismic parameters of ferropericlase in the lower mantle. American Mineralogist, 2019. 104(2): p. 262–275. DOI: 10.2138/am-2019-6656.

[50] Birch, F., Finite strain isotherm and velocities for single-crystal and polycrystalline NaCl at high pressures and 300 K. Journal of Geophysical Research, 1978. 83(B3): p. 1257–1268. DOI: 10.1029/JB083iB03p01257.

[51] Duffy, T.S. and D.L. Anderson, Seismic velocities in mantle minerals and the mineralogy of the upper mantle. Journal of Geophysical Research, 1989. 94(B2): p. 1895–1912. DOI: 10.1029/JB094iB02p01895.

[52] Watanabe, H., Thermochemical Properties of Synthetic High-Pressure Compounds Relevant to the Earth's Mantle. High-pressure research in geophysics, 1982: p. 441–464. DOI: 10.1007/978-94-009-7867-6_34.

[53] Boehler, R. and J. Ramakrishnan, Experimental results on the pressure dependence of the Grüneisen parameter: A review. Journal of Geophysical Research, 1980. 85(B12): p. 6996–7002. DOI: 10.1029/JB085iB12p06996.

[54] Boehler, R., Adiabats of quartz, coesite, olivine, and magnesium oxide to 50 kbar and 1000 K, and the adiabatic gradient in the Earth's mantle. Journal of Geophysical Research: Solid Earth, 1982. 87(B7): p. 5501–5506. DOI: 10.1029/JB087iB07p05501.